Simultaneous formation of Si and Ge nanocrystals in SiO_2 by one step ion implantation

P.K. Giri [a,*], R. Kesavamoorthy [b], S. Bhattacharya [a], B.K. Panigrahi [b], K.G.M. Nair [b]

[a] *Department of Physics, Indian Institute of Technology Guwahati, Guwahati 781039, India*
[b] *Materials Science Division, Indira Gandhi Center for Atomic Research, Kalpakkam 603102, India*

Abstract

Germanium (Ge) and silicon nanocrystals (NCs) are synthesized by one step Ge ion implantation into thermally grown SiO_2 layers and subsequent annealing. X-ray diffraction and Raman scattering studies on implanted samples reveal that Ge nanocrystals of sizes 4–13 nm are formed embedded in SiO_2 for Ge fluence in the range 3×10^{16} to 2×10^{17} cm^{-2}. At high fluence ($\geq 1 \times 10^{17}$ cm^{-2}) and annealing temperature of 950 °C, in addition to these Ge NCs, Si NCs are formed at the interface between Si and SiO_2 layer as a result of ion impact. Optical Raman spectra show a distinct peak at ~503 cm^{-1} corresponding to the Si NCs. The average size of the Si NCs are smaller than the average size of the Ge NCs. Implications of our results are discussed in the light of the versatility of the ion-beam technique for the synthesis of varieties of embedded NCs.
© 2005 Elsevier B.V. All rights reserved.

Keywords: A. Nanocrystals; B. Ion implantation; C. Germanium; D. Raman scattering

1. Introduction

Over the last decade, there has been growing interest in synthesizing semiconductor nanocrystals (NCs) in SiO_2 because of their interesting optical [1] and electronic properties [2]. Several methods can be used to fabricate such structures [3,4]. Among these, ion-beam synthesis has received considerable interest because of its ease and simplicity in growing NCs of varying size. Both Si [5] and Ge [6] NCs have been grown by implanting either Si$^+$ or Ge$^+$ ions into thermally grown SiO_2 films and subsequent annealing at temperatures of 800 °C or higher in inert gas environment. Due to their compatibility with microelectronics, both these group IV materials in nanocrystalline phase offer a variety of applications in optoelectronic [7] and electronic memory [8] devices. However, growth of two different species of NCs by one-step ion implantation has not been reported. In this letter, we describe the synthesis of both Ge and Si NCs in a single sample by one step Ge$^+$ ion implantation. It is shown that at high fluences, in addition to Ge NCs in the SiO_2 matrix, Si NCs form near the SiO_2/Si interface. Implications of this novel finding are discussed in the context of versatility of ion-beam synthesis of NCs.

2. Experimental details

Before implantation, SiO_2 films were grown by wet oxidation of Si (1 0 0) wafers. The oxide thickness was measured to be 250 nm by spectroscopic ellipsometry. The films were implanted with 300 keV Ge ions at fluences 3×10^{16} (Ge1), 1×10^{17} (Ge2) and 2×10^{17} (Ge3) ions/cm^2, respectively, to grow nanocrystals of different sizes. The Monte Carlo code SRIM [9] predicts that the implanted Ge ions have a mean projected range of 205 nm and a projected range straggling of 62 nm. The SRIM calculation reveals that a major fraction of the Ge ions are deposited at the SiO_2/Si interface. Embedded Ge and Si NCs were formed when the as-implanted samples were annealed at 800 and 950 °C in argon gas atmosphere. We characterize these samples by X-ray diffraction (XRD) and Raman spectroscopy to identify the Ge and Si NCs. Raman spectra were recorded in the backscattering geometry using a vertically polarized 488 nm Ar$^+$ laser. XRD spectra were recorded using a powder diffractometer system in grazing incidence mode. Rutherford backscattering spectrometry (RBS) measurements were performed using collimated 2 MeV He$^+$ ion beams from a Tandem accelerator.

* Corresponding author. Tel.: +91 361 2582703; fax: +91 361 2690762.
  E-mail address: giri@iitg.ernet.in (P.K. Giri).
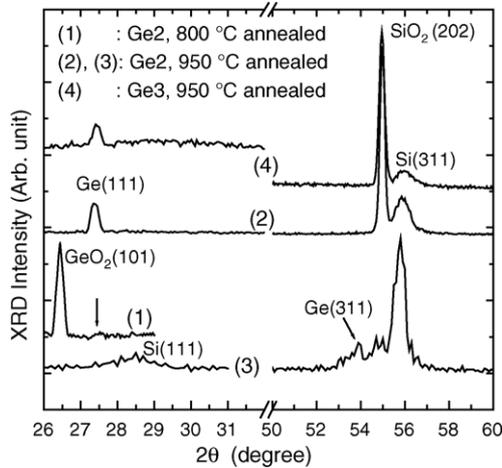
Fig. 1. Grazing incidence X-ray diffraction spectra of Ge implanted and annealed SiO2/Si layer. Curve 1: annealing at 800 °C for Ge2 and curves 2, 3: annealing at 950 °C for Ge2, curve 4: annealing at 950 °C for Ge3. Curves 1, 2 and 4 are obtained with grazing angle of 2° and curve 3 is obtained with grazing angle of 3°.

3. Results and discussion

Fig. 1 shows a set of grazing incidence XRD spectra on Ge2 and Ge3. Curves 1, 2 and 4 were obtained with grazing angle of 2° and curve 3 was obtained with an angle of 3°. Curve 1 is for Ge2 sample post annealed at 800 °C, curves 2 and 3 are for Ge2 post annealed at 950 °C and curve 4 is for Ge3 post annealed at 950 °C. The strong Bragg peak at 26.44° and a weak peak at ~27.4° (shown with arrow) in curve 1 correspond to GeO$_2$ (1 0 1) and Ge (1 1 1) NCs, respectively [10]. Due to the very small size of the NCs in 800 °C annealed sample, Ge related peak is broad and weak in the XRD spectra. After 950 °C annealing, the Ge (1 1 1) peak became distinct due to larger size of the NCs as shown in curves 2 and 4. Curve 3 shows both Si (1 1 1) and Ge (3 1 1) peaks after annealing at 950 °C. It is found that the broad Si (1 1 1) peak at 28.4° and Si (3 1 1) peak at 55.9° occur in Ge2 and Ge3 samples only after annealing at 950 °C. The broad Si peaks are the signatures of the formation of Si NCs. If the Si (1 1 1) or Si (3 1 1) peak width is used to estimate the size of Si NCs using Debye–Scherrer formula, then the mean size of the NCs comes out to be ~8 nm. This is similar to the estimated average size of Ge NCs using low frequency Raman spectrum (Table 1 vide infra). However, due to relatively large

Table 1
Ge nanocrystallite size (mean) as a function of ion fluence and annealing temperature (T_a)

Sample no.	Ge$^+$ fluence (cm^{-2})	Ge NC size (nm)	
		$T_a = 800$ °C	$T_a = 950$ °C
Ge1	3×10^{16}	4.0 ± 0.1	6.1 ± 0.1
Ge2	1×10^{17}	5.4 ± 0.1	13.0 ± 0.1
Ge3	2×10^{17}	4.1 ± 0.1	9.2 ± 0.1

Mean size (diameter) of the NCs is determined from the low frequency Raman scattering data (see text). Uncertainty in size is calculated from the uncertainty in the peak position as obtained from line shape fitting.

concentration of Ge in SiO$_2$ layer, average size of the Ge NCs is expected to be larger than the size of the Si NCs. We think that X-ray method gives an overestimate of the size due to possible effect of size distribution and strain of the NCs on the spectral line shape. Therefore, actual size of the Si NCs would be smaller than the size estimated from Debye–Scherrer formula.

The optical Raman spectra of Ge1 sample shown in Fig. 2 reveal peaks at 304 and 435 cm^{-1} corresponding to scattering from optical phonons involving Ge–Ge and Si–Ge stretching motions, respectively [11]. The strong peak at 521.6 cm^{-1} arises from the Si substrate, and weak peaks at ~230 and ~253 cm^{-1} are signatures of Ge related components. Similar Raman spectra have been observed by Wu et al. [12] in Ge$^+$ implanted SiO$_2$. Single crystalline Ge wafers show a Raman peak at 301.1 cm^{-1}. We expect a downshift of the NC Ge Raman peak due to phonon confinement effect, but we observed a small upshift in the Raman peak position. Though the reason for this upshift is not clear, it may be caused by the compressive stress exerted on Ge NCs by the surrounding SiO$_2$ matrix because of the interface where the nearest neighbor distance in SiO$_2$ is much smaller than that in Ge [12].

To determine the size of the Ge NCs, low frequency Raman scattering (LFRS) measurements were performed on these samples. LFRS modes arise from the surface acoustic phonons of Ge NCs at the interface between the crystallite and the embedding dielectric matrix, and its frequency is inversely proportional to the size of the NCs [13]. LFRS of 800 °C annealed samples show a peak at 21.2 cm^{-1} in Ge1 and 15.7 cm^{-1} in Ge2 sample. After 950 °C annealing, these peaks shift to 13.8 and 6.5 cm^{-1}, respectively, indicating an increase in the size of NCs. The average diameter of the NCs estimated from LFRS varies from 4 to 13 nm depending on the ion fluence and annealing temperature and is shown in Table 1. It is clear from Table 1 that Ge NCs grow in size with the increase of the ion fluence and the annealing temperature. It is well known that NCs fabricated by ion implantation show a wide distribution of size and the measured size is the average of the sizes present in the matrix. In the present study, NCs were biggest at 1×10^{17} ions/cm^2 after 950 °C post-annealing. Details of the LFRS analysis are presented elsewhere [14].
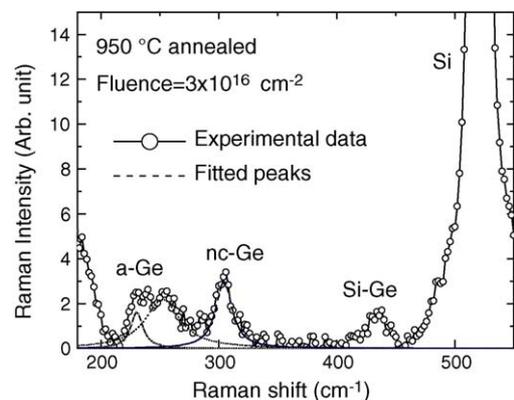
Fig. 2. Optical Raman spectra of the 950 °C annealed sample implanted with Ge ions. Experimental data is shown with symbol + solid line and the dashed line is a fit to Lorentzian line shapes. Bonds responsible for the modes are indicated.
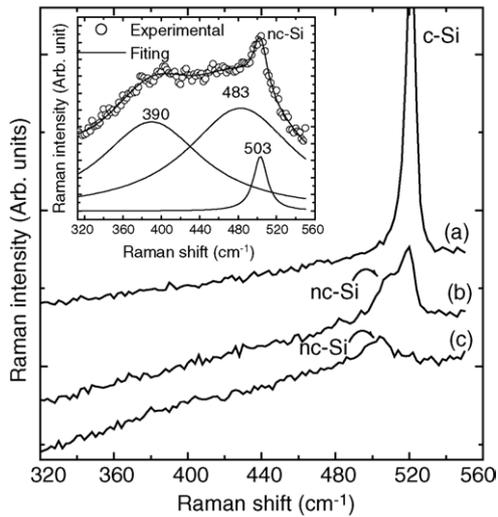
Fig. 3. Optical Raman spectra of the 950 °C annealed samples: (a) Ge1, (b) Ge2 and (c) Ge3. Signature of Si NCs is indicated with arrow for Ge2 and Ge3 samples. The inset shows the background subtracted Raman spectra with constituent peaks fitted to Lorentzian line shapes. Peak positions are denoted by the corresponding wave numbers.

Fig. 4. (a) Rutherford backscattering (RBS) spectra of Ge ion-implanted SiO_2 layer after annealing at 950 °C. Experimental spectrum is shown with solid line and simulated spectrum is shown with dashed line. (b) Ge depth profile as obtained form fitting of RBS spectra from Ge1 sample and the simulated profile as obtained from SRIM calculation for comparison. Vertical dashed line shows the SiO_2/Si interface.

Fig. 3 shows a set of Raman spectra for 950 °C annealed Ge1, Ge2 and Ge3 samples. At low fluence, a sharp peak is observed at 521 cm^{-1} due to the Si substrate. At higher fluence ($\geq 1 \times 10^{17}$ cm^{-2}), the Si peak intensity diminishes and broadens due to ion damage. Fig. 3 shows that in addition to the crystalline Si peak, another peak emerges at ~503 cm^{-1} in Ge2 sample and this peak becomes prominent at a fluence 2×10^{17} (Ge3). The inset of Fig. 3 shows the spectra of Ge3 sample and the constituent peaks after subtracting the background. The 503 cm^{-1} Raman peak is attributed to Si NCs [15], which form as a result of ion impact near the Si/SiO$_2$ interface. The broad peaks at ~483 and ~389 cm^{-1} are attributed to amorphous Si and Si–Ge bonds, respectively [11].

During the high fluence implantation, 300 keV Ge$^+$ ions reach the SiO$_2$/Si interface and deposits energy to the surrounding Si atoms. A major fraction of the displaced Si atoms are segregated in the SiO$_2$ layer making it a silicon rich oxide layer. Subsequent heat treatment of the Si supersaturated layer at 950 °C induces the nucleation and growth of the Si NCs near the Si/SiO$_2$ interface [16]. These Si NCs are detected by XRD and Raman studies only for high fluence implanted samples. To support our view, we performed two additional measurements. Firstly, we compare the results of SRIM calculation of the Ge profile and the measured Ge profile using Rutherford backscattering spectrometry (BRS) technique for the Ge1 and Ge3 samples. RBS measurement on the 950 °C annealed Ge3 sample shows (Fig. 4) that Ge profile has a dip near the SiO$_2$/Si interface, implying that there is reduction in Ge concentration near the SiO$_2$/Si interface after annealing. It is likely to result from the supersaturation and clustering of the displaced Si atoms near the interface caused by the ion-bombardment. These clustered Si atoms grow to Si NCs during post-implant annealing and Ge atoms density is effectively reduced in this region as seen from Fig. 4. Heat treatment

at lower temperature (800 °C) or implantations at low fluence do not induce segregation of Si atoms and thus no Si NC peak is detected. Secondly, to substantiate further about the mechanism of NC formation, we implanted 100 keV Ar ions at a fluence of 5×10^{16} ions/cm^2 on SiO$_2$ layer [thermally grown on Si (1 0 0) substrate] and annealed at 950 °C under inert gas atmosphere. Low frequency Raman scattering studies on this sample show Raman peaks corresponding to acoustic phonon modes of some NCs. Since Si is the only species that can form NCs in the Si/SiO$_2$ interface, our studies confirm that very small Si NCs are formed as a result of Ar ion bombardment in the SiO$_2$ layer and subsequent annealing. Our preliminary studies show a LFRS peak at ~28.0 cm^{-1} in this sample that would correspond to a Si NC of size ~5–6 nm. Further studies are under progress to determine the quality of the NCs formed by such implantations.

Since the phonon confinement, particle size distribution and the strain in the NCs all contribute to the line shape broadening of the Raman spectra of Ge implanted SiO$_2$ layer, the mean size of the Si NCs cannot be estimated from the Raman line width. The Si NCs yielding a Raman peak at ~503 cm^{-1} corresponds to a peak shift of about 18 cm^{-1} from that of the bulk Si. If the downshift is due to phonon confinement alone, neglecting the strain effect, the estimated Si NC size would be ~1.4 nm [15]. Although this certainly underestimates the size, Si NC sizes are expected to be smaller than the size of the Ge NCs (as determined from LFRS studies), primarily due to the low density of the Si atoms available for nucleation and growth.

In a separate study, time resolved photoluminescence (PL) measurements along with steady state PL measurements on Ge implanted samples suggested that both the Ge NCs and the defects in SiO$_2$ matrix contribute to the light emission characteristics [17]. In these samples, the density of the Ge NCs is much larger than that of Si NCs. LFRS studies show that observed low frequency modes (spheroidal and torsional) correspond to one species of NCs [14,18] i.e. Ge NCs only. The broad Si (1 1 1) peak in Fig. 1 indicates the presence of very small Si NCs and their corresponding scattering cross-section is very low in LFRS spectra. Hence, the LFRS analysis is not affected by the presence of small Si NCs. Similarly, ultrafast PL decay dynamics of the Ge nanocrystals suggests that Ge NCs primarily contribute to the observed dynamics in the nanosecond time-scale. This is in contrast to the slow decay dynamics usually exhibited by Si NCs. It is to be understood that Si NCs grow as a byproduct of the Ge$^+$ implantation process in SiO$_2$. This is made possible by choosing the energy of the implanting species such that a large fraction of the deposited ion energy is used for displacing the Si atoms and mixing at the Si/SiO$_2$ interface [16]. By subsequent heat treatment ion damage is recovered and Si NCs grow in size. Since, the energy deposition and displacement of Si ions in Si/SiO$_2$ interface can be caused by any heavy ion species with sufficient energy, this effect is expected to be independent of the ion species. Our preliminary studies of 100 keV Ar ion implantation on SiO$_2$ verify this proposition. We anticipate that ion implantation method would be useful for synthesis of NCs of desired species by choosing the appropriate substrates and suitable thermodynamic conditions.

4. Conclusions

We have synthesized Ge and Si NCs in the same SiO$_2$ layer by single step ion implantation. By choosing an appropriate energy and fluence of the implanted Ge$^+$ ions and post-implant annealing, Si NCs are formed in the SiO$_2$ layer, in addition to the Ge NCs in the SiO$_2$ matrix. XRD and Raman studies confirm the formation of both Ge and Si NCs in samples implanted with high fluence ($\geq 1 \times 10^{17}$ cm^{-2}) and annealed at 950 °C. Si NCs are believed to form as a result of radiation-induced transfer energy to Si ions and their nucleation and growth under suitable thermodynamic conditions. Our preliminary studies with inert gas ions have shown results favorable to this proposition. Our results imply that under suitable thermodynamic conditions any energetic heavy ion species could be implanted at the interface of any immiscible bilayer system to produce NCs of desired species.

Acknowledgements

References

[1] R.T. Collins, P.M. Fauchet, M.A. Tischler, Phys. Today 50 (1997) 24.
[2] Y.C. King, T.J. King, C. Hu, IEEE Trans. Electron. Devices 48 (2001) 696.
[3] M. Nogami, Y. Abe, Appl. Phys. Lett. 65 (1994) 2545.
[4] D.C. Paine, C. Caragianis, T.Y. Kim, Y. Shigesato, T. Ishahara, Appl. Phys. 62 (1993) 2842.
[5] S. Guha, M.D. Pace, D.N. Dunn, I.L. Singer, Appl. Phys. Lett. 70 (1997) 1207.
[6] K.S. Min, K.V. Shcheglov, C.M. Yang, H.A. Atwater, M.L. Brongersma, A. Polman, Appl. Phys. Lett. 68 (1996) 2511.
[7] H. Rong, R. Jones, A. Liu, O. Cohen, D. Hak, A. Fang, M. Paniccia, Nature 433 (2005) 725.
[8] W.K. Choi, W.K. Chim, C.L. Heng, L.W. Teo, V. Ho, V. Ng, D.A. Antoniadis, E.A. Fitzgerald, Appl. Phys. Lett. 80 (2002) 2014.
[9] www.srim.org/SRIM/SRIM2003.htm.
[10] M. Zacharias, P.M. Fauchet, Appl. Phys. Lett. 71 (1997) 380.
[11] Mi.I. Alonso, K. Winer, Phys. Rev. B 39 (1989) 10056.
[12] X.L. Wu, T. Gao, X.M. Bao, F. Yan, S.S. Jiang, D. Feng, J. Appl. Phys. 82 (1997) 2704.
[13] E. Duval, A. Boukenter, B. Champagnon, Phys. Rev. Lett. 56 (19862052).
[14] P.K. Giri, R. Kesavamoorthy, B.K. Panigrahi, K.G.M. Nair, Solid State Commun. 136 (2005) 36.
[15] R.K. Soni, L.F. Fonseca, O. Resto, M. Buzaianu, S.Z. Weisz, J. Luminol. 83–84 (1999) 187.
[16] V. Ovchinnikov, V. Sokolov, S. Franssila, Microelectron. J. 34 (2003) 579.
[17] P.K. Giri, R. Kesavamoorthy, B.K. Panigrahi, K.G.M. Nair, Solid State Commun. 133 (2005) 229.
[18] N.N. Ovsyuk, E.B. Gorokhov, V.V. Grischenko, A.P. Shebanin, JETP Lett. 47 (1988) 298.